AN EXPERIMENTAL INVESTIGATION OF THE ELECTRONIC STRUCTURE OF THE F^+-CENTER IN SrO

By

BRYCE T. JEFFRIES

Bachelor of Science

Central State University

Edmond, Oklahoma

1976

Submitted to the Faculty of the Graduate College
of the Oklahoma State University
in partial fulfillment of the requirements
for the Degree of
MASTER OF SCIENCE
December, 1979

TO

LINDA

AND

LYDIA

AN EXPERIMENTAL INVESTIGATION OF THE

ELECTRONIC STRUCTURE OF THE

F+-CENTER IN SrO

Thesis Approved:

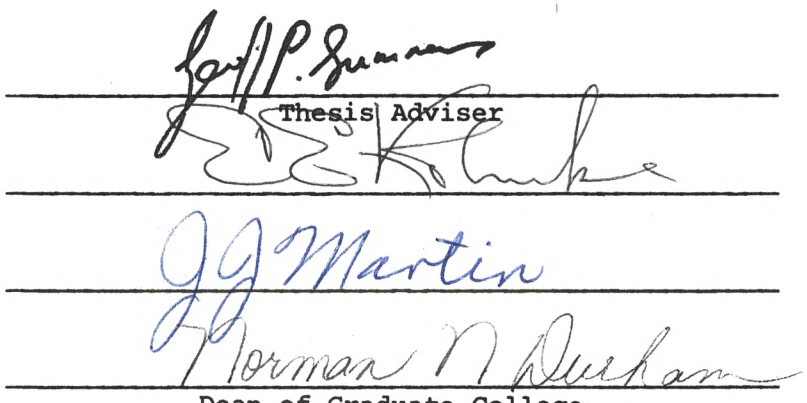

Thesis Adviser

Dean of Graduate College

ACKNOWLEDGMENTS

The author wishes to express his appreciation to his major adviser, Dr. Geoffrey P. Summers, for his guidance and help in completing this thesis. I also want to thank him for providing an atmosphere where I was expected to search things out on my own.

Thanks are given to the Physics Faculty for their friendship and many interesting discussions.

Thanks is given to Joel Brewer for his friendship and for the many discussions we have had trying to figure problems out.

Special thanks to my wife who has supported me with her love and friendship.

My best thanks are given to God who continually shows His love for me.

Finally appreciation is given to the Department of Energy for the financial support provided.

TABLE OF CONTENTS

TABLE

LIST OF FIGURES

CHAPTER I

INTRODUCTION

I. Introduction

A major area of interest in solid state physics is the study of point defects. A certain kind of point defect called a color center involves crystal lattice irregularities that absorb light in the UV, infrared, and visible regions of the spectrum.

II. The F-Type Center

A particular type of color center is the F-type center. In an F-type center an anion vacancy is created in the crystal. Since the anion, an oxygen ion in SrO for instance, leaves behind a positively charged vacancy the point defect can trap a number of electrons depending upon the charge of the defect and the availability of electrons in the crystal. The F-center in SrO has trapped two electrons and the F+-center has trapped one electron.

There are two main methods of introducing color centers into crystals. They can be produced by irradiating the crystal with particles such as electrons, charged ions, or neutrons (1,2) or they can be produced by additive coloration, where the crystal is grown with an abundance of the metallic ion present (3). Ionizing radiation such as x-radiation and gamma radiation will not produce anion or cation vacancies

in SrO but can have the effect of redistributing charge within the crystal. In SrO particle irradiation only produces F+-centers. F-centers are produced only by additive coloration. This ability of separately producing F and F+-centers makes their experimental analysis much simpler than is the case in CaO, for example.

Neutrons are electrically neutral and do not have a coulombic interaction with atoms so they can penetrate deeply into the crystal. Also their energy is dissipated through knock-on collisions making them very effective in producing point defects. Because they impart a large amount of energy in collisions, localized areas of great damage can be produced since the atom moved now has a large kinetic energy and interacts coulombically with its neighboring atoms. Electron and charged ion irradiation produces defects in a different manner due to long range coulombic interactions. Because of this charged ions do not penetrate very deeply but do their damage near the surface. Electrons of a given energy have a much higher velocity than an ion of the same evergy. For this reason they penetrate comparatively deeply into a crystal and produce a more uniform damage throughout the crystal.

As described above, the mass, velocity, and electronic charge of the incident particle determines how much damage is produced. Another factor is that singly isolated oxygen ions appear to be unstable in the SrO crystal lattice and can easily recombine with a lattice vacancy. This fact partially explains why incident electrons even well above threshold energy cause so little damage. The heavier particles by displacing more oxygen atoms in a local area allow them to form into clusters which are fairly stable. So neutrons, protons, and other ions produce stable damage in SrO but electrons are inefficient at producing

damage even at low temperatures.

One factor that determines whether F or F+-centers are predominant is the number of electron traps present in the crystal. These traps limit the number of electrons available to populate the oxygen vacancies. Another factor that may have some effect is that when oxygen atoms form into stable clusters each oxygen retains only one of the extra electrons it carried away. This other electron would then be free to return to the point defect producing an F+-center (4). This effect would not be important in additively colored crystals.

The body centered cubic structure of SrO is shown in Figure 1. The structure is common to most alkali halides and alkaline earth oxides. The structure is formed by placing alternately O^{2-} and Sr^{2+} ions at each corner of a simple cube. The bonds are comparatively ionic with the lattice constant being 5.1695 Å (5) and its melting point being 2415 ^{o}C (6).

The F+-center has several characteristics that permit measurements to be made. It is paramagnetic since only one electron is present. This allows for electron paramagnetic resonance (EPR, or ESR) measurements on the ground state. Two related experiments that study the unrelaxed excited state are faraday rotation (FR) and magnetic circular dichroism (MCD) (7) . In FR the indices of refraction for right and left circularly polarized exciting light is different and the effect seen is the rotation of the plane of plane polarized light. In MCD the absorption of right and left circularly polarized exciting light is different. To study the relaxed excited state, photoluminescence, photoconductivity, and fluorescence lifetime measurements are made. Photoluminescence measurements are used to find the temperature

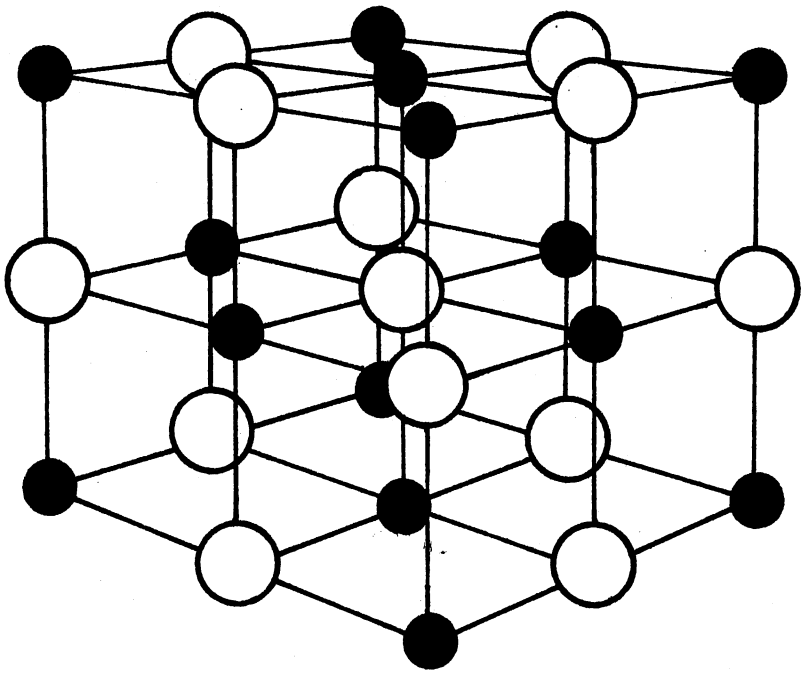

Figure 1. Crystal Structure of SrO

dependence of the fluorescence intensity of the crystal defects. Photoconductivity measurements are used to measure the depths of traps and to measure the depths of excited states of defects below the conduction and valence bands. Fluorescence lifetime measurements are used to investigate the temperature dependence of different escape processes from an excited state.

III. Experimental Studies

In identifying the F+-center in SrO several experimental studies have been conducted. Bessent, Cavenett, and Hunter (8) through the use of FR at 4.2 K have identified the F+-center absorption band at 3.0 eV. Verification of their work was accomplished by Modine et al. (9) using a double resonance technique which is a combination of ESR and MCD. The MCD technique is more accurate than FR and gave the F+-center absorption at 3.1 eV. The next study was done by Modine et al. (10). Their corresponding optical density and MCD data verified the absorption at 3.1 eV. Hughes and Webb (11) measured the shape and moments of the F+ absorption band and also suggested that a temperature dependent emission band at 500 nm (2.5 eV) was due to the F+-center.

Measurements on the relaxed excited state were made by Feldott and Summers (1) using photoconductivity. Their measurements showed that by exciting the crystal at 3.1 eV the photoconductivity increased sharply from 63 K to 100 K and then decreased for higher temperatures. Using a two level model for the F+-center they obtained a thermal activation energy of 0.12 eV for exciting electrons into the conduction band. Next Feldott et al. (2) performed luminescence and lifetime measurements. A luminescence band centered at 2.5 eV with a half-width of 0.34

eV at 5 K and a fluorescence lifetime of 420 ns at 5 K were assigned to the F+-center. The theoretical model they presented is shown by the configuration coordinate diagram in Figure 2. Excitation occurs from the $^2A_{1g}$ state to the $^2T_{1u}$ state. The $^2A^*_{1g}$ state lies above the $^2T_{1u}$ state in absorption but after lattice relaxation the $^2A^*_{1g}$ state ends up lower than the $^2T_{1u}$ state. By setting the absorption energy at 3.1 eV they obtained a value of 0.2 eV for the energy gap between the $^2A^*_{1g}$ state and the conduction band. The energy gap between the $^2T_{1u}$ and $^2A^*_{1g}$ states after lattice relaxation was found to be 0.06 eV and the emission energy was calculated to be 2.5 eV. The calculations showed that the $^2T_{1u}$ relaxed excited state was strongly coupled to A_{1g} and T_{2g} vibrational modes. Coupling the $^2T_{1u}$ state to the T_{2g} modes produced a Jahn-Teller lowering of the energy of the $^2T_{1u}$ state so that it became almost degenerate with the $^2A^*_{1g}$ state. Possible further mixing of the $^2T_{1u}$ and $^2A^*_{1g}$ states by odd parity T_{1u} vibrational modes made the transition from the $^2A^*_{1g}$ state to the $^2A_{1g}$ ground state not strictly forbidden. These results qualitatively explain the relatively long radiative lifetime of the F+-center.

IV. Objective of the Study

In this study photoluminescence and fluorescence lifetime experiments were conducted in order to obtain additional information to compare with the theoretical model and experimental results above. Chapter II presents the experimental apparatus and procedure. Chapter III contains the experimental results and analysis and Chapter IV contains the discussion of the experimental results. A model is

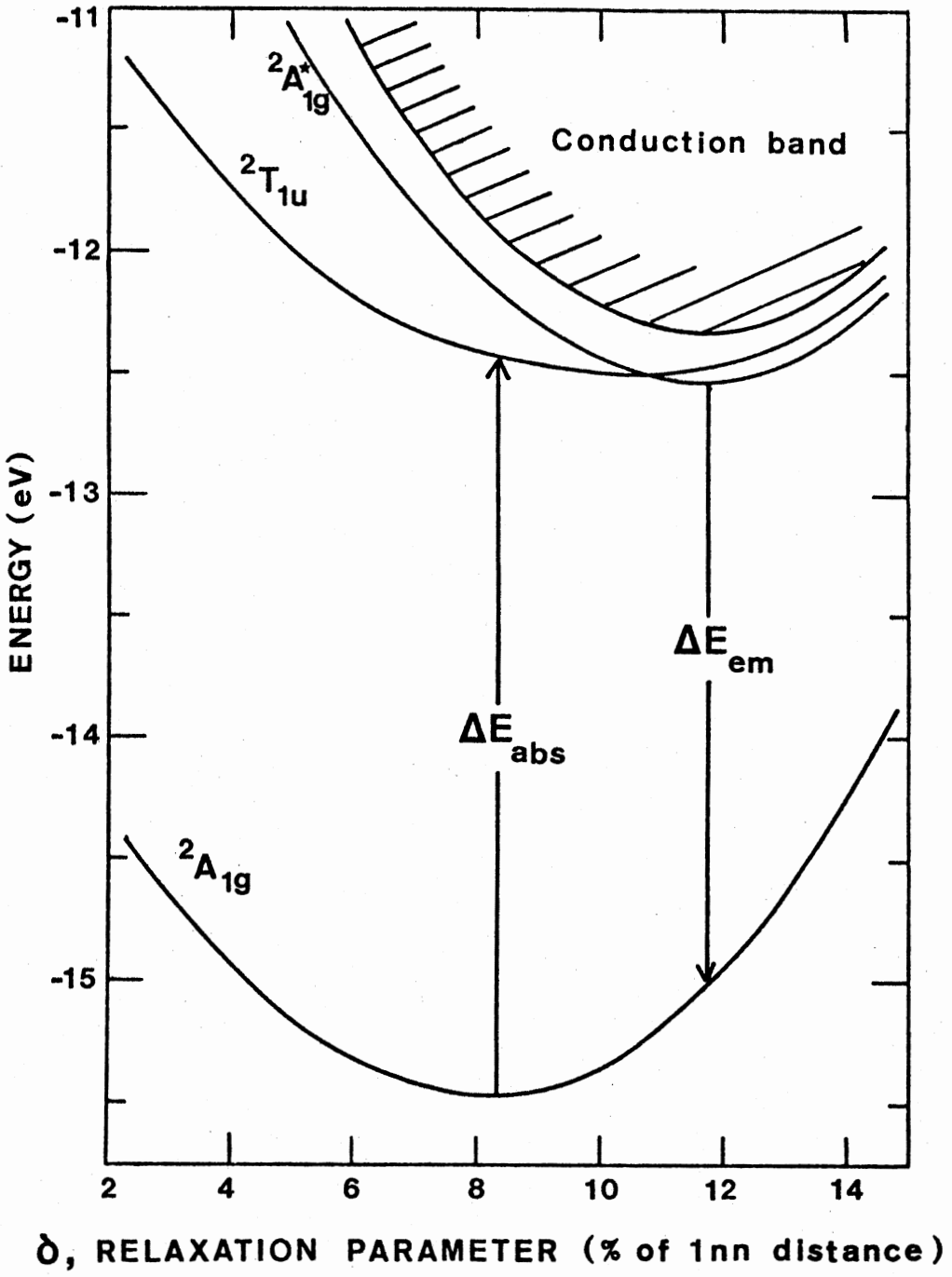

Source: Feldott et al. (2)

Figure 2. Configuration Coordinate Diagram for SrO

presented that is consistent with known theoretical information about the F+-center and which also successfully explains the experimental results.

CHAPTER II

EXPERIMENTAL APPARATUS AND PROCEDURE

I. Introduction

In this thesis the determination of the electronic structure of the F+-center in SrO is the sought outcome. Information to accomplish this was obtained from measuring as a function of temperature the luminescence intensity and the radiative lifetime of the F+-center fluorescence. It is worth recalling that the optical band occurs at 400 nm (3.1 eV) and the photoluminescence band occurs at 500 nm (2.5 eV). In this chapter the details of the experimental equipment and procedure are described.

II. Sample Preparation

The SrO crystal used in these experiments was obtained from Dr. Y. Chen of Oak Ridge National Laboratory (ORNL) and is the same crystal used by Feldott et al. (2) in their experiments. It was grown and irradiated with fast neutrons at ORNL. The approximate dimensions of the crystal are 1.19 mm by 14.54 mm by 9.32 mm. Because the alkaline earth oxides except for MgO are hygroscopic, the SrO crystal was stored in parafin oil. When preparing the crystal for an experiment the surface to be irradiated with exciting light was polished with six micron alumina paper and then was cleaned with trichloroethane. Next it

was attached to the cold finger of the cryostat with silicon based high vacuum grease. The crystal was then masked with aluminum foil so the light would be absorbed and reemitted only from the polished surface. The sample chamber of the cryostat was then evacuated.

III. Optical Density

Optical density measurements were made with a Cary 14 Spectrophotometer. Since the measurements were made at 77 K the SrO crystal was attached by a spring loaded copper plate to the cold finger of a cryostat. The measurements were made over a spectral range from 250 nm to 650 nm (5 eV to 2 eV) and filters were used so that the optical density, OD, could be measured up to 4.8. The optical density is given by the relation:

$$OD = \log_{10} \frac{I_o}{I} \tag{1}$$

where

I_o is the incident intensity of the reference light

I is the transmitted light intensity.

The intensity of transmitted light is given by:

$$I = I_o \exp(-\alpha d) \tag{2}$$

where

α is the absorption coefficient

d is the crystal thickness.

This gives the relationship between the absorption coefficient and the optical density as:

$$\alpha = 2.303\left(\frac{OD}{d}\right)\ cm^{-1}. \qquad (3)$$

IV. Temperature Measurements

The temperature range covered in these experiments ranged down to 5 K so a gold-chromel thermocouple was used since it allowed for accurate measurements. The thermocouple was attached to the sample area on the cold finger of the cryostat. The reference junctions were maintained at 0 ^{o}C and attached by copper wires to a Keithley Model 171 Digital Multimeter. Since the cryostat did not have a temperature control the measurements were made while the cryostat warmed up. The cryostat had inner and outer cooling chambers so the outer heat shield was maintained at 77 K with liquid nitrogen during measurements below 77 K. This prevented the cold finger from warming up too fast. In measurements above 77 K the outer heat shield could be cooled to 77 K and then its temperature allowed to rise with the rest of the system. The rate of warming up could be sped up by blowing air into the two chambers. The rate of temperature change was approximately 3 K every five minutes except around 45 K where it was almost three times as large.

V. Photoluminescence

A block diagram of the photoluminescence apparatus is shown in Figure 3. The exciting light was emitted by a 150 watt xenon lamp powered by an Illumination Industries Model CA150 Power Supply and then focused on the sample with a lens. All of the lenses used in these experiments were made from S-1 UV grade quartz because of its flat

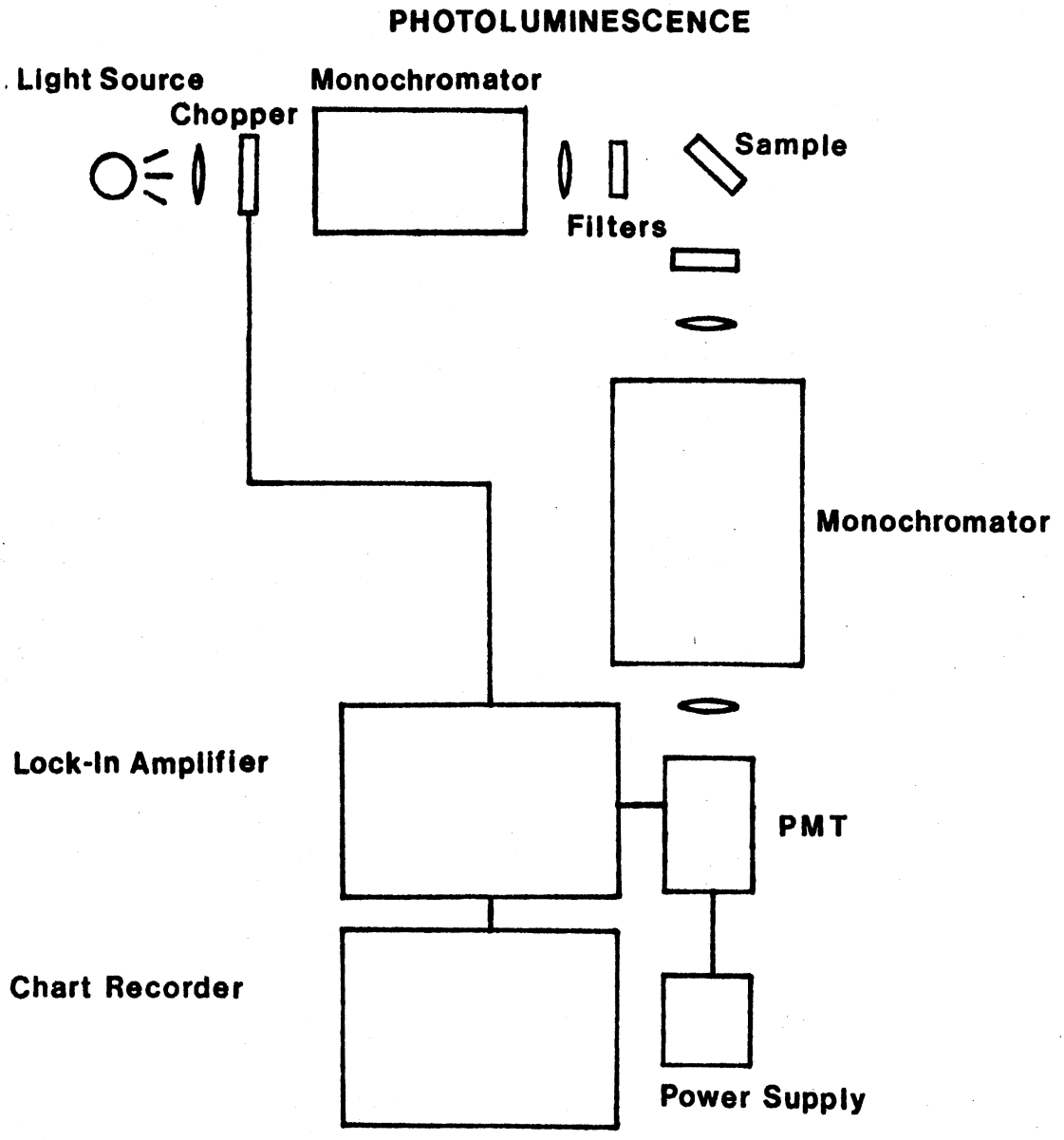

Figure 3. Photoluminescence Apparatus

responce from 250 nm to 2000 nm. The light passed through a Princeton Applied Research (PAR) Mechanical Light Chopper and was dispersed with a Spex 1670 Minimate .22 m Monochromator with a linear dispersion of 40 Å. The grating was blazed at 3000 Å and had 1200 groves/mm, and the wavelength readout was accurate to ±2 nm. Its entrance and exit slits were set at 1.25 mm and the grating was set to select 385 nm (3.2 eV) light. This setting was chosen instead of 400 nm (3.1 eV), the optical band peak of the F+-center in SrO, for several reasons. It was not far off the excitation peak and the excitation spectrum does not change appreciably over the temperature range from 5 K to 150 K (7). Also it still gave a strong signal and allowed a better resolution of the photoluminescence band in its high energy region. Upon exiting from the monochromator the exciting light passed through a Corning CS7-60 band-pass filter. It cut off stray light at approximately 400 nm and prevented the excitation system from interfering with the detection system. It also served to keep the intensity of the exciting light low enough to prevent any possible bleaching of the emitted light. The light then was directed onto the sample. After exiting from the cryostat the emitted light first passed through a CS3-74 sharp cut filter. This filter cut off around 404 nm (3.1 eV) and prevented any of the excitation light from entering the detection system. The emitted light was then dispersed by a GCA McPherson 218 .3 m Monochromator with its slits set at 1 mm. The monochromator had a linear dispersion of 26.5 Å and contained a grating blazed at 3000 Å with 1200 groves/mm. The dispersed light from the monochromator was detected by an RCA C31034 Photomultiplier Tube (PMT) cooled to -30 ^{o}C by a water cooled Pacific Photometric Institute Thermoelectric Photomultiplier Housing Model 3463 powered by a

Power Supply/Temperature Controller Model 33. This PMT has an almost uniform responce from 300 nm to 800 nm. The current from the photomultiplier was amplified by a PAR Model 181 Current Sensitive Preamplifier. This signal was then fed into a PAR Model 128A Lock-In Amplifier. A reference signal from the mechanical chopper was used by the lock-in amplifier to produce a dc output signal proportional only to that part of the preamplifier signal which was synchronous with the chopper's signal. This output was fed into a Heath Model SR-205 Single Pen Chart Recorder. The recorder and the McPherson monochromator were synchronized to record signal strength as a function of wavelength.

In order to analyse the data the photoresponce of the detection system had to be determined as a function of wavelength. The system was set up as in Figure 3 except that a 75 watt quartz halogen lamp was directed into the mechanical chopper and then into the McPherson monochromator. The intensity of this light was recorded as a function of the wavelength. At 5 nm intervals this resulting curve intensity was divided into the relative number of photons emitted by the lamp. The relative number of photons were calculated from a blackbody curve for a quartz halogen lamp. The transmittance of the CS3-74 filter was combined with the above to arrive at the relative number of photons per system responce. The results are shown in Figure 4.

VI. Fluorescence

A block diagram of the fluorescence apparatus is shown in Figure 5. The exciting light was produced by a Xenon Corporation Model 437A Nanolamp with a Model CA150 Power Supply. The nanolamp emitted a light pulse with a rise time of 10 ns, a half-width of 20 ns, and a repetition

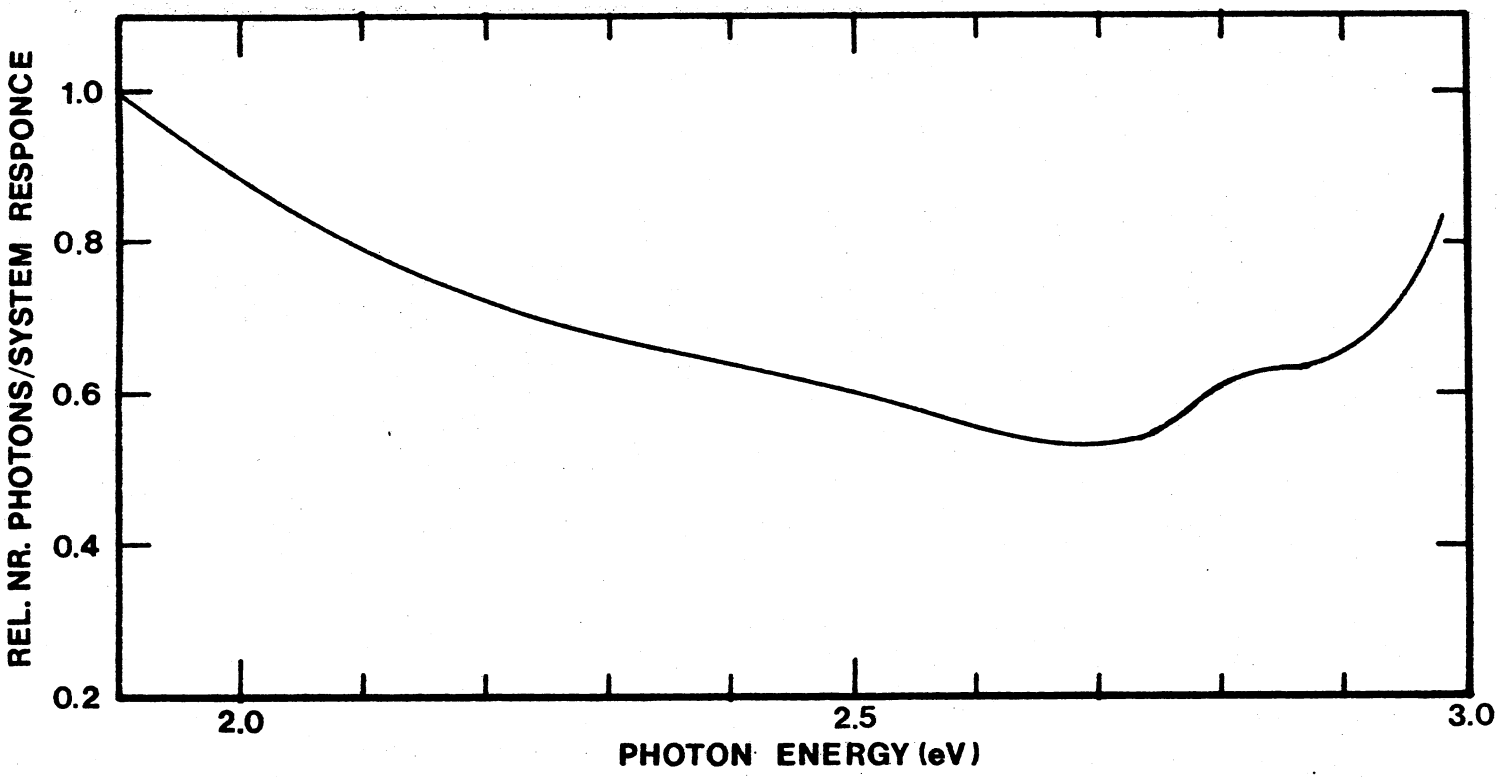

Figure 4. Intensity Normalization Curve

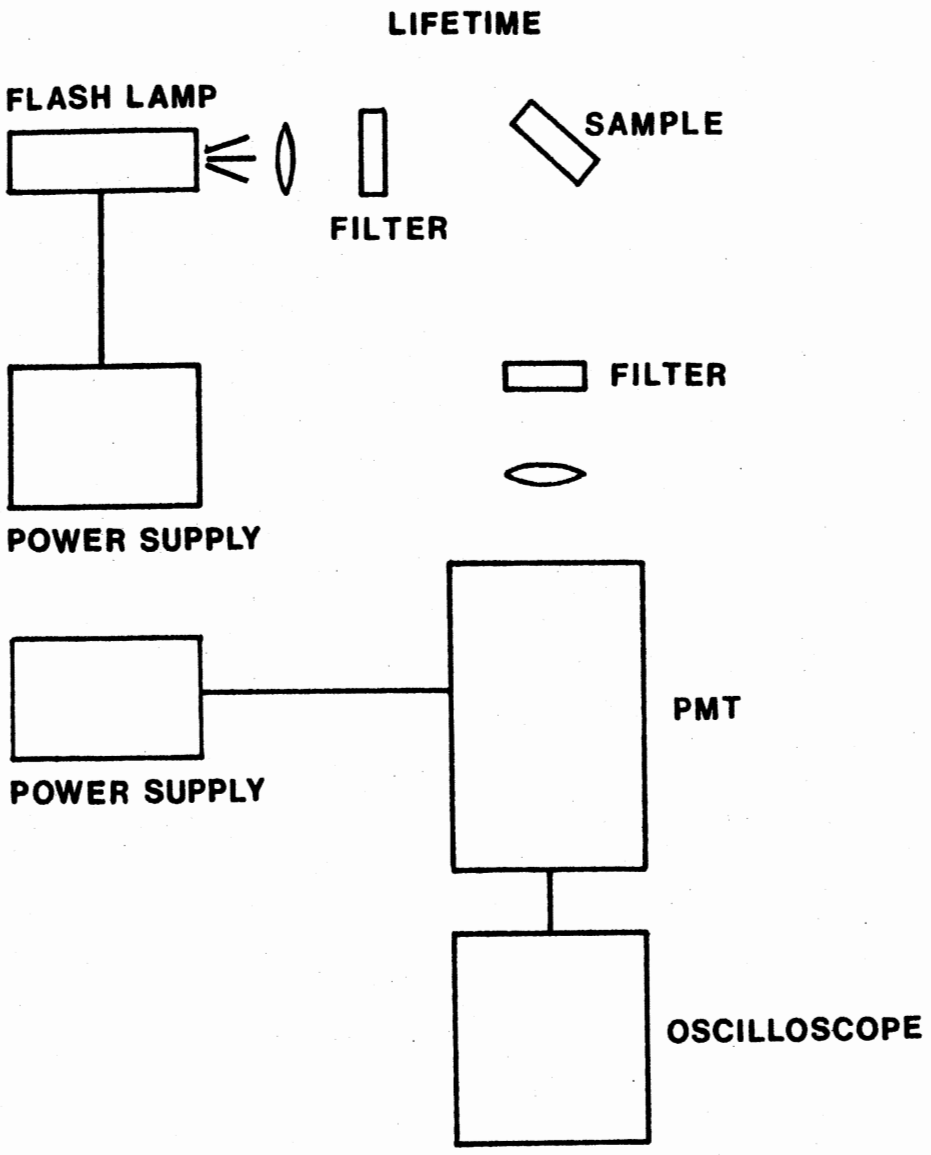

Figure 5. Lifetime Apparatus

rate of approximately thirty flashes a second. The exciting light first passed through an Oriel Corporation G522-4047 interference filter which has a peak transmittance at 4051 Å with a half-width of 82 Å. The exciting light then passed through either a CS 7-51 or a CS7-59 bandpass filter. They cut off the light at approximately 395 nm (3.14 eV) and 480 nm (2.59 eV) respectively. The bandpass filters were used to cut down the intensity of the light, cut out stray light, and allow different parts of the excitation spectrum to reach the crystal. The light emitted from the crystal next passed through either a CS3-73, CS3-71, or CS3-70 sharp cut filter. Their cut offs were at approximately 420 nm (2.96 eV), 475 nm (2.61 eV), and 490 nm (2.53 eV) respectively. The CS3-73 was used in conjunction with the CS7-51 and either the CS3-70 or the CS3-71 was used with the CS7-59. By using these different combinations, different parts of the emission spectrum could be analysed to see the effect on the intensity of different lifetimes. The light was then detected by an EMI 9813-B PMT. The PMT's output was fed into a Tektronix 7603 Wideband Oscilloscope by a shielded coaxial cable to eliminate effects caused by the sparking of the nanolamp. The oscilloscope contained a 7B50A Timebase Module and a 7A16A Amplifier Module and the input was shunted with a 50 ohm resistor to produce a system responce of 25 ns. A Model C-50 Oscilloscope Camera was used to photograph the screen. The photographs were projected on a wall with an opaque projector and their images were traced on graph paper.

CHAPTER III

EXPERIMENTAL RESULTS

I. Introduction

In this chapter the experimental results will be presented and analysed and compared with previous experimental and theoretical results. The end results will suggest a model for the F+-center which will be developed in Chapter IV.

II. Optical Density

In Figure 6 is presented the optical absorption spectra at 77 K of the neutron irradiated SrO crystal and nonirradiated SrO crystal obtained from Spicer Ltd. The main feature of the neutron irradiated crystal spectrum is the asymmetric optical band centered at 3.1 eV (400 nm) with an optical density (OD) of 3.1. This is the F+ optical band that has been previously reported (1,8). As is true for particle irradiated SrO, no F band is seen at 2.5 eV. There are other peaks at 2.1, 2.7, 3.9, and 4.6 eV and a small sharp peak at 2.25 eV. The nonirradiated crystal shows no F or F+ optical band but mainly a rising background as it gets closer to the band edge. The neutron irradiated crystal shows a much higher background absorption possibly related to aggregated damage regions in the sample.

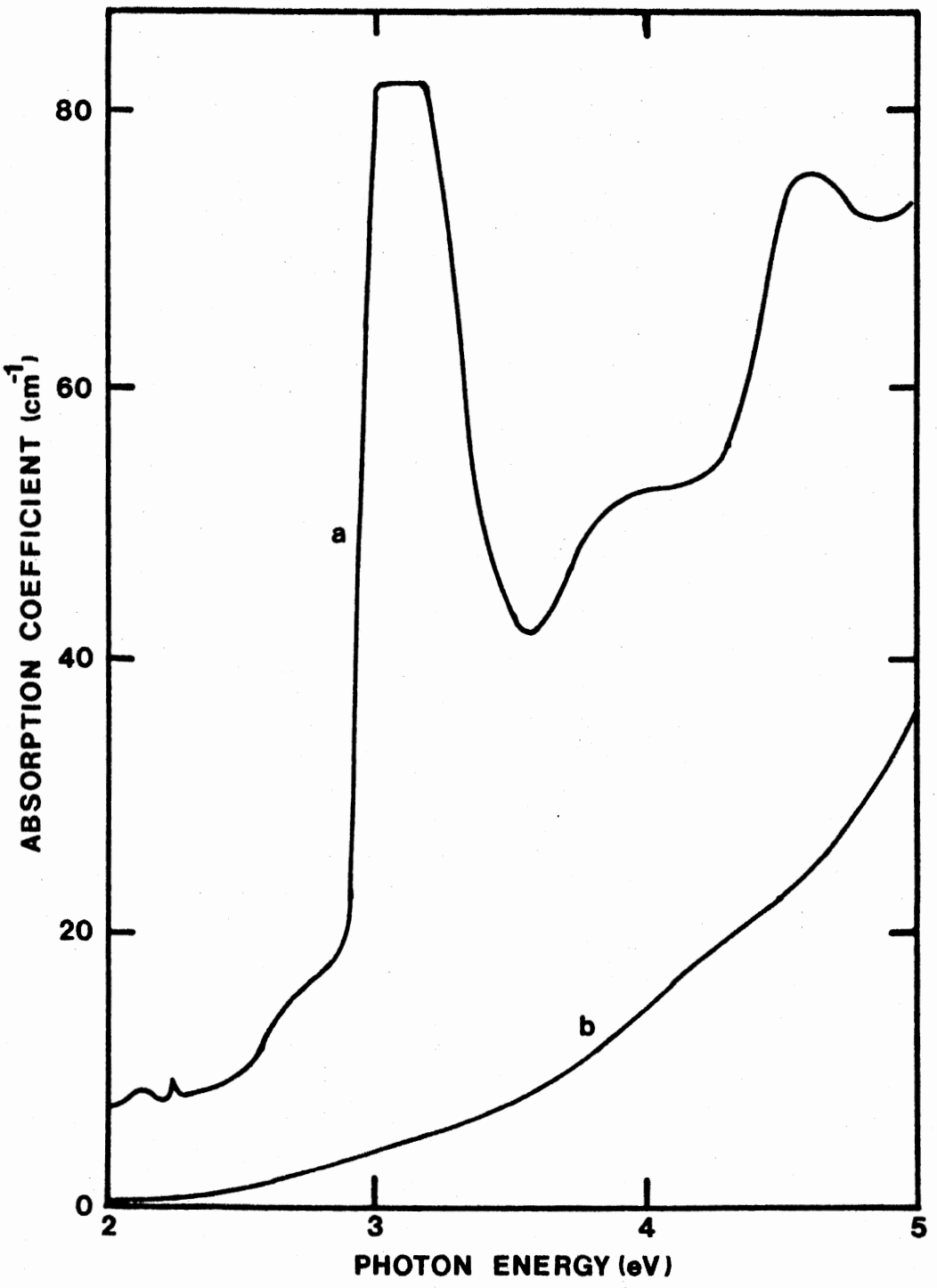

Figure 6. Optical Density of SrO. Fast neutron irradiated with F+ optical peak at 3.1 eV, Curve a; nonirradiated from Spicer Ltd., Curve b

III. Temperature Dependence of Photoluminescence

In this section a presentation of the temperature dependent photoluminescence of the SrO crystal will be given. The measurements were made as described in Chapter II. The excitation light spectrum was selected by setting the Spex Monochromator at 385 nm (3.2 eV) and also using a Corning CS7-60 bandpass filter. A 150 watt xenon lamp was directed through these components. The light emitted from the crystal passed through a CS3-74 sharp cut filter before entering the detection system. This set up allowed us to look at the photoluminescence up to an energy of about 3.1 eV (404 nm).

The measurements were taken at approximately 10 K intervals as the crystal slowly warmed up. The data was recorded as a function of wavelength. It was read from the chart paper at intervals of 0.05 eV from 1.90 eV (653 nm) to 3.00 eV (414 nm). This was then multiplied by the correction curve shown in Figure 4 to give the relative emission. In Figure 7 is shown a plot of every other measurement over a temperature range from 5 K to 151 K. At 5 K the F+-center band has a peak located at 2.5 eV and a half-width of 0.34 eV. These values are in agreement with the previous experimental results of Feldott et al. (2). The 2.5 eV band also has a low energy tail evident over the whole temperature range making the curve slightly asymmetric. Starting at 5 K the intensity of the F+-center decreases significantly with increasing temperature and is practically zero at 151 K. Around 60 K another band becomes apparent at 2.7 eV (460 nm). This band increases in intensity until it reaches 130 K and then decreases slowly as the temperature increases. It should be mentioned here that the photoconductivity due to F+-centers

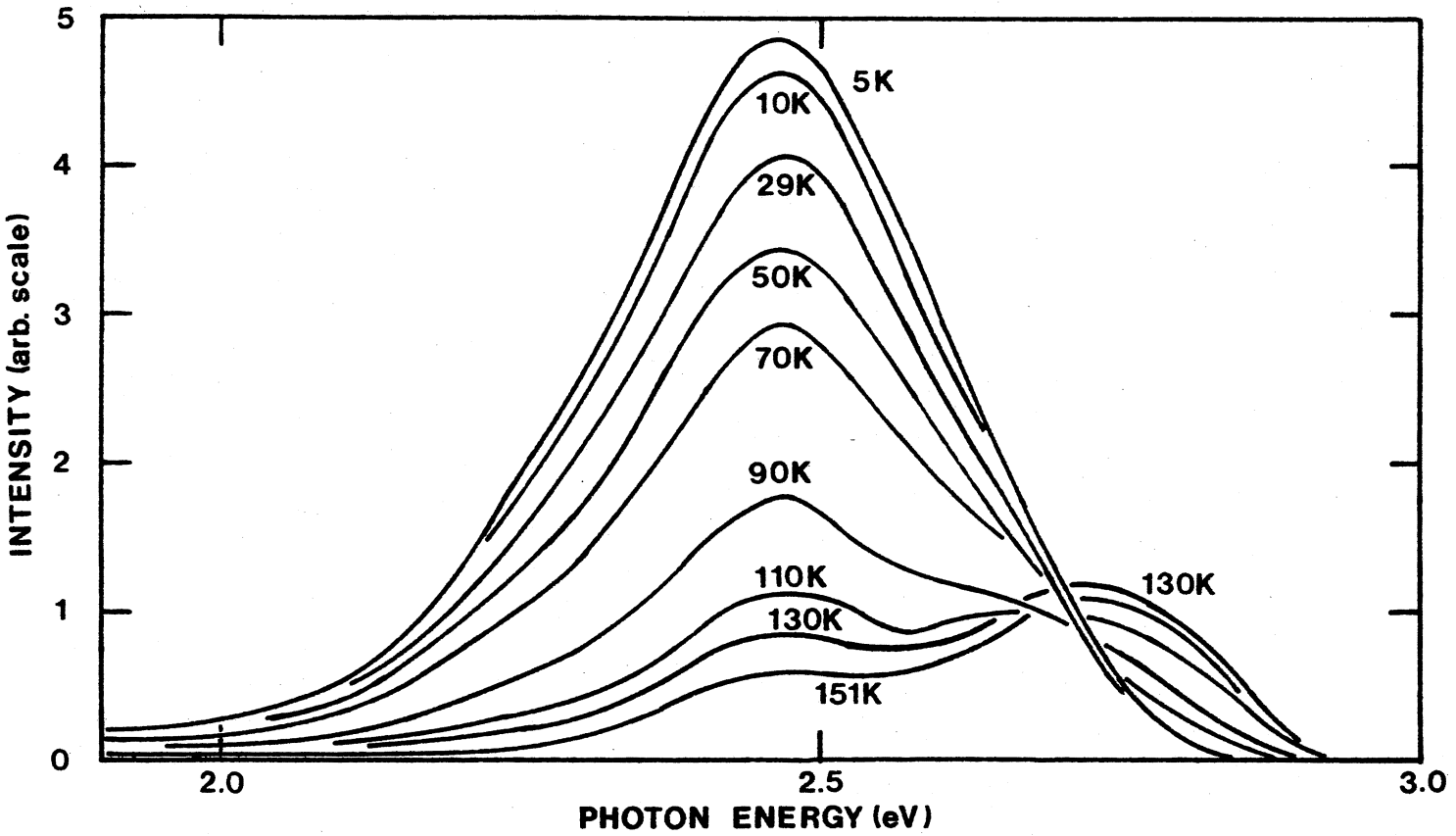

Figure 7. Fluorescence Intensity. Spectral dependence of fluorescence intensity from 5 K to 151 K

is found to increase with increasing temperature starting around 60 K also. The 2.7 eV band has been observed in nonirradiated SrO when the 2.5 eV band is not present and is thus attributed to an impurity in the crystal (13). It is also asymmetric and has a low energy tail.

Since SrO is hygroscopic measurements were made to determine if the hydroxide ions that bond to the crystal had affected the measurements. A nonirradiated SrO crystal was exposed to water vapor over a two day period. The photoluminescence measurements were made but no significant effect was observed over the range from 1.90 to 3.00 eV.

The presence of the 2.7 eV band makes the analysis of the F+ luminescence intensity as a function of temperature complicated. A method will be shown below that enables a resonable analysis of the intensity to be made. The intensity of the F+-center appears to disappear much faster as the temperature rises above 70 K. These results are consistent with a model where the electrons can at least be thermally excited into the conduction band or can return to the ground state by radiative recombination. A more detailed model will be presented in Chapter IV.

IV. Fluorescence

In this section the lifetime of the fluorescence of the F+-centers in SrO is presented. The measurements were made as described in Chapter II. An Oriel G522-4047 (3.07 eV) interference filter and an air gap spark nanolamp along with either a Corning CS7-51 or CS7-59 bandpass filter were used for exciting the F+-centers. The emitted light passed through either a CS3-70, CS3-71, or CS3-73 sharp cut filter before entering the detection system.

The data photographed from the oscilloscope screen was very noisy

and it was not possible to get accurate measurements of the lifetimes. In Figure 8 is a plot of four representative lifetimes. Also plotted is the 25 ns responce of the system. The top two traces have long tails which are not shown. The long lived part of the lifetime has been associated with the F+-center (2). The computer fitted lifetimes decrease from 429 ns at 5 K to 140 ns at 140 K. The short lifetimes also seem to show a temperature dependence in going from 75 ns to 40 ns. Difficulty in reading especially this part of the data makes the temperature dependence of the short lifetime suspect. This difficulty also affects the accuracy in determining the long lifetime. Jeffries and Summers et al. (12) conclude that this lifetime component which is almost independent of temperature may come from an impurity band in the same spectral region as the F+-center. This lifetime may come from the supposed impurity band at 2.7 eV. As has already been described the temperature dependence of the lifetime of F+-centers in proton irradiated SrO has been measured. The proton irradiated Sro data is plotted as the dots in Figure 9 with the neutron irradiated data plotted as the squares. The solid error bars go with the proton irradiated data and the dashed error bars go with the neutron irradiated data. The fitted curve was obtained from the model developed in Chapter IV. The curve is a good fit to the data.

V. Temperature Dependence of the F+ Fluorescence

To do a detailed study of the F+ fluorescence intensity as a function of temperature the effect of the 2.7 eV band must be subtracted from the fluorescence intensity. In order to do this the data was

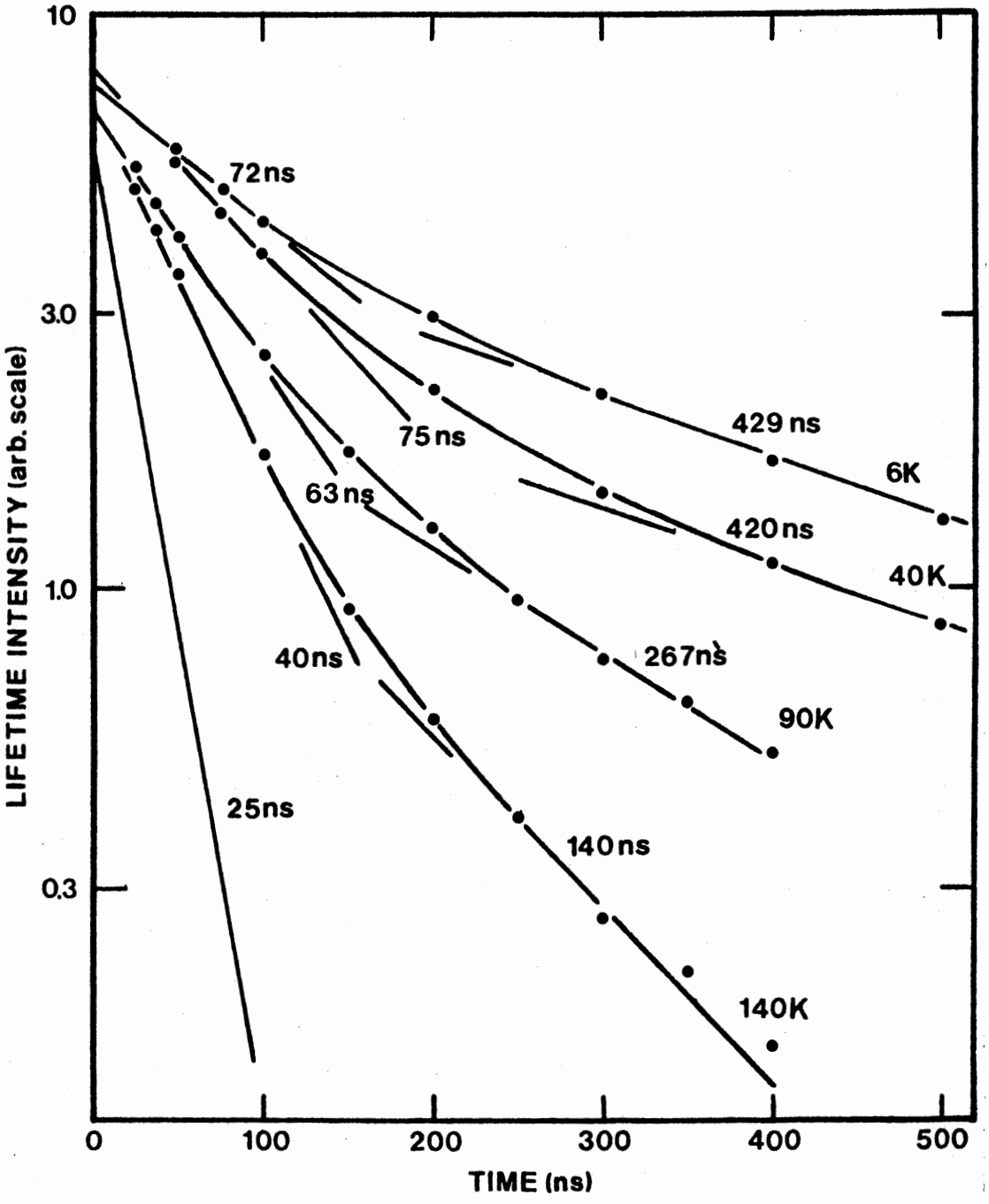

Figure 8. Lifetimes

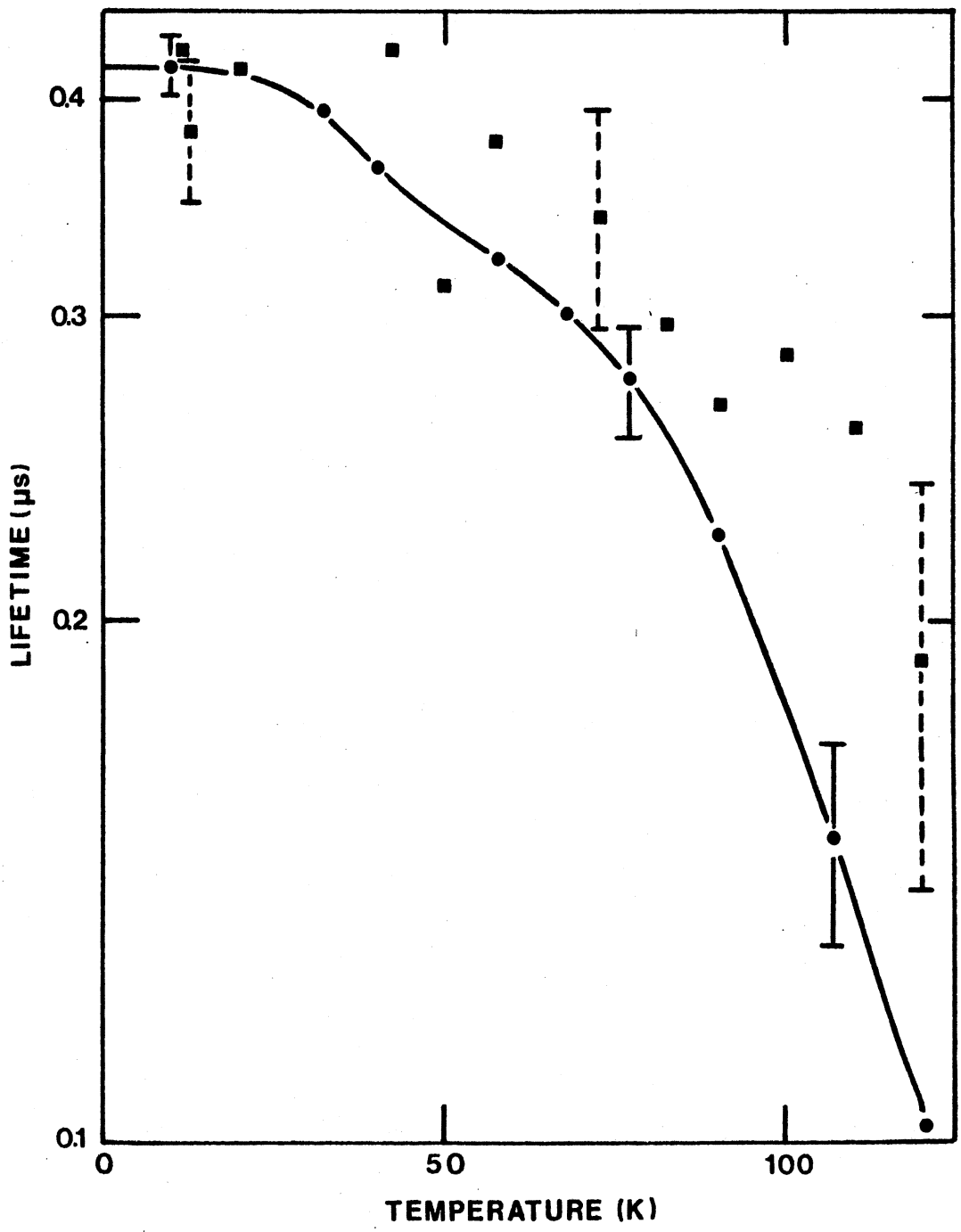

Figure 9. Lifetime Versus Temperature. Dots are proton irradiated SrO lifetime data. Squares are neutron irradiated SrO lifetime data

fitted to a double Gaussian curve by a PDP 11/10 Minicomputer. The function used to do this is:

$$I = K_1 \exp\{-2.772(\frac{E_1-E}{H_1})^2\} + K_2 \exp\{-2.772(\frac{E_2-E}{H_2})^2\} \quad (4)$$

with K_1 and K_2 the heights at the band peaks, H_1 and H_2 the half-widths, and E_1 and E_2 the photon energy at the peak heights for the 2.5 and 2.7 eV bands respectively. E is the energy parameter and I is the intensity. The program used is a Fortran library program on the university's IBM-370 computer. It uses their Patrn (OSU Computer Center classification) search routine and does a linear least squares fit. It was determined that a single Gaussian best fitted the data from 5 K to 40 K. A double Gaussian was then used from 50 K to 151 K. Since the low energy tail has to be ignored, it was not fitted with the rest of the data. The part not fitted ranged on the energy scale from 1.90 to 2.25 eV. In Figure 10 is a plot of the 5 K and 90 K curves. The dots and circles are the data recorded at 0.05 eV intervals. The solid lines are the computer fits with the 90 K curve also being broken down into its two components. The 5 K curve overestimates the data around 2.8 eV and underestimates it at the peak. The amount of the low energy tail not included amounts to approximately 8 per cent of the total area. This is probably uniform until the temperature reaches 110 K. For higher temperatures the area under the 2.5 eV curve starts to contain a significant part of the asymmetric 2.7 eV band thereby making its value larger than it should be. The main concern here is that a good approximation to the area under the F+-center curves be found and this fit does give a good approximation of this area. Since the data has been normalized the area

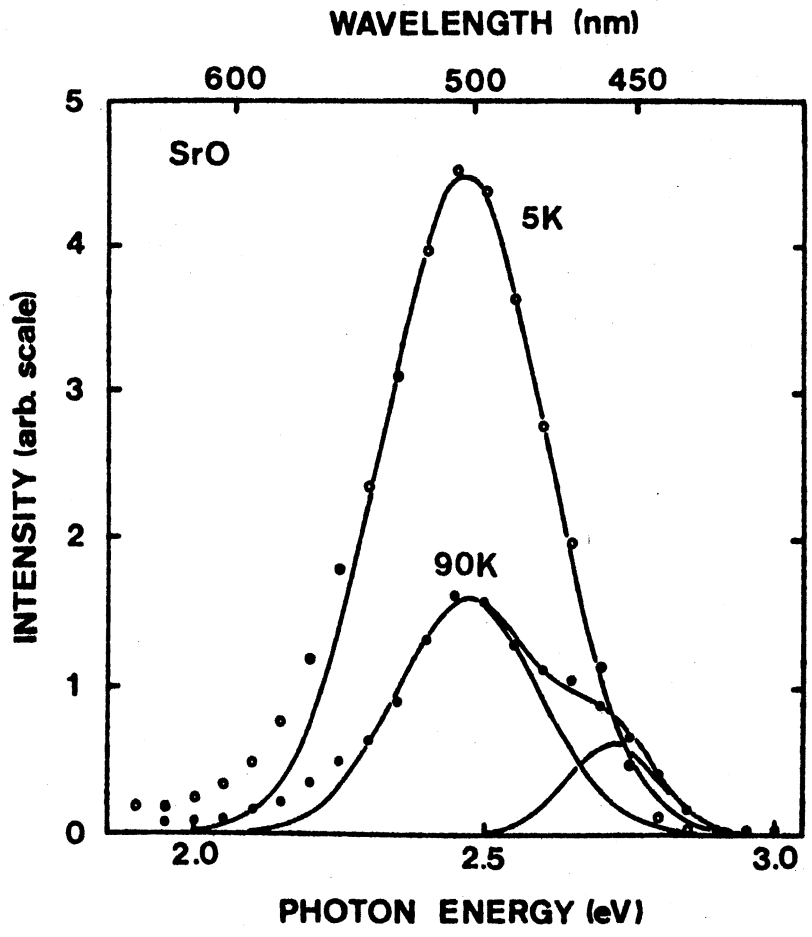

Figure 10. Gaussian Fits of Fluorescence Intensity. Gaussian fits to 5 K and 90 K curves with the 90 K curve broken into its two Gaussian components

under the curves gives a measure of the quantum efficiency for the radiative decay of the excited F+-center. Figure 11 shows the temperature dependence of the F+ fluorescence using the area of the Gaussians over the temperature range from 5 K to 151 K. The circles give the F+-center fluorescence intensity and the fitted curve is the fit of the data to a model which is developed in Chapter IV. The relative intensity of the 2.7 eV fluorescence is shown as dots. The most important feature of the fluorescence intensity is the two stage thermal quenching of the F+-center. The first stage is from 5 K to 60 K and the second is from 60 K to 151 K. Also both the 2.7 eV band and the photoconductivity coincide with the second stage of quenching.

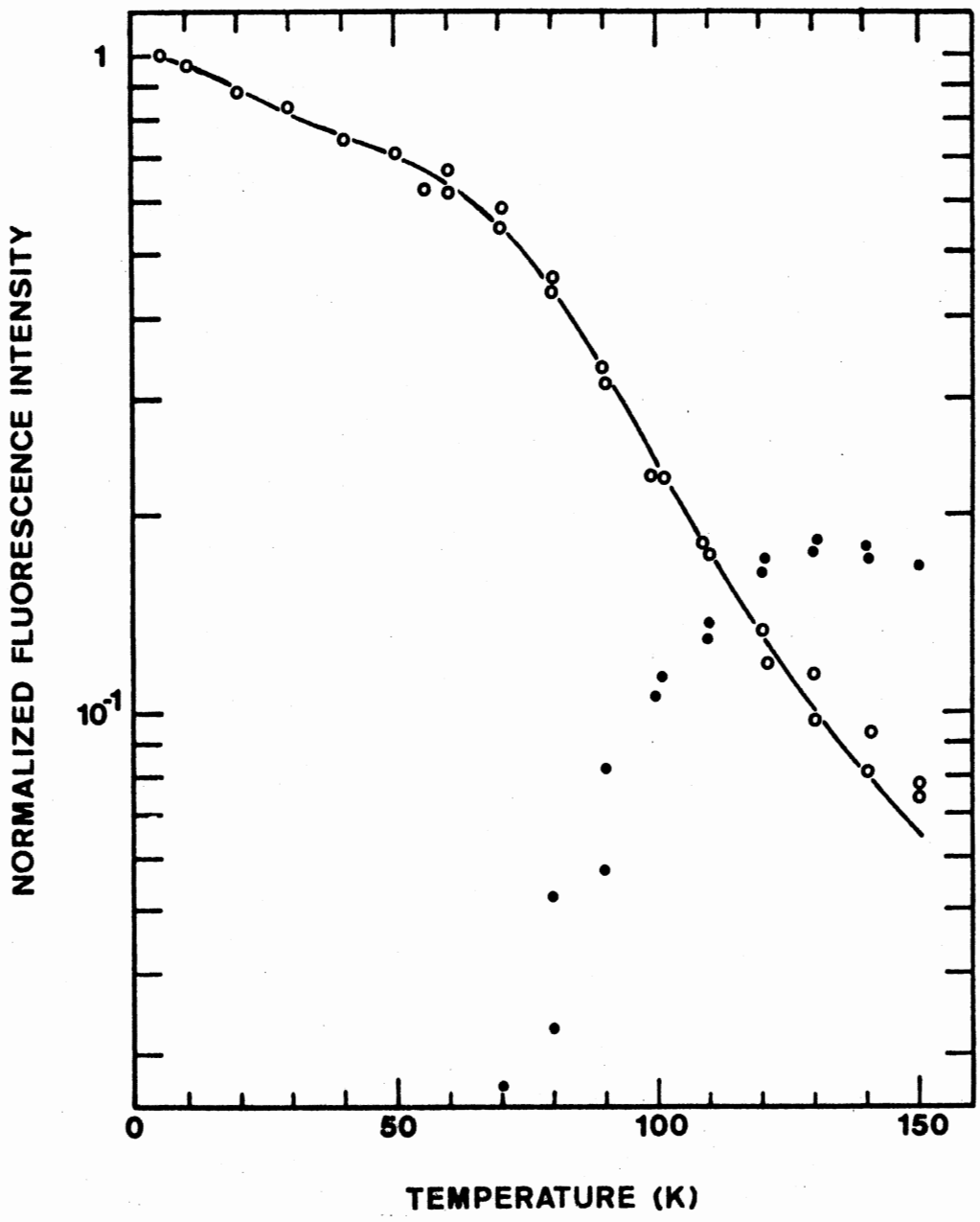

Figure 11. Temperature Dependence of the Fluorescence Intensity. Double quenching of the F+-center with computer fit. 2.7 eV band occuring at 60 K

CHAPTER IV

DISCUSSION

From looking at the two stage thermal quenching of the fluroescence intensity in Figure 11 it is clear that a two level model will not fit the data. For the data to fit a two level model the fluorescence intensity would have to remain constant until the electrons could escape into the conduction band. Then as the intensity would decrease photoconductivity could be measured. But we have a decrease in intensity before photoconductivity starts so a more complicated model must be considered. The configuration coordinate diagram in Figure 2 suggests that a three level model should be tried because it has in its relaxed excited state a lower $^2A^*_{1g}$ state separated by a fraction of an eV from an upper $^2T_{1u}$ state. From the theoretical calculations the two states are separated by 0.06 eV and the $^2A^*_{1g}$ state is 0.2 eV below the conduction band. The absorption energy was assumed to be 3.1 eV and the emission was then calculated to be 2.5 eV (2). Further calculations made the states almost degenerate by Jahn-Teller lowering of the $^2T_{1u}$ state and mixed the two states thereby eliminating the forbidden nature of the transition from the $^2A^*_{1g}$ to the $^2A_{1g}$ state.

The three level model that fits the experimental data is shown in Figure 12. The radiative transitions are shown as straight lines and and the nonradiative transitions are shown as wavy lines. The $^2A_{1g}$, $^2T_{1u}$, and $^2A^*_{1g}$ states are represented by levels 0, 1, and 2 respectively

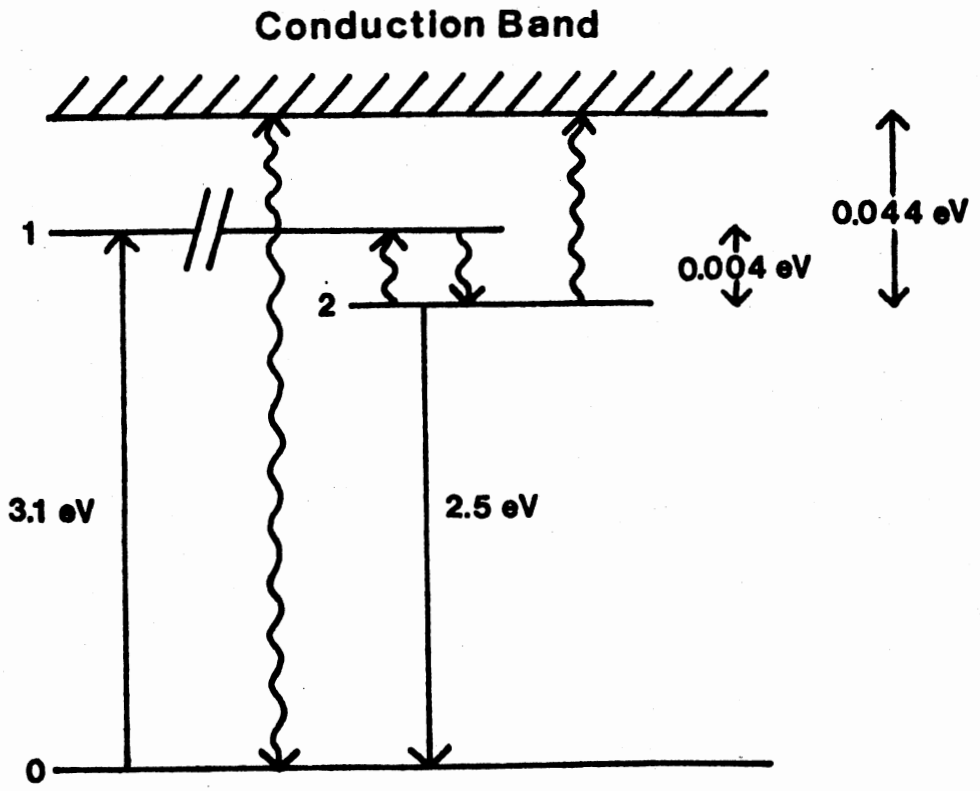

Figure 12. F+-Center Model for SrO. Three level model with optical transition from level 2, non-radiative recombination from level 1, and thermal excitation into the conduction band from level 2

with populations of n_0, n_1, and n_2. The conduction band is represented as level 3. Excitation light raises electrons from level 0 to level 1 at the rate $k_{01}n_0$. After the F+-center relaxes emission occurs from level 2 to level 0 with a rate constant k_{20}. Between levels 1 and 2 there is an up rate k_{21} and a down rate k_{12}. The rates k_{13} and k_{23} are thermal ionization rates into the conduction band.

The main feature of this model is that the transition from level 1 to level 0 has to be nonradiative. This is necessary to explain the thermal quenching of the fluorescence intensity from 5 K to 60 K.

The rate equations that describe the time rate of change of levels 1 and 2 are:

$$\frac{d\,n_1}{dt} = \dot{n}_1 = k_{01}n_0 + k_{21}n_2 - (k_{10} + k_{12} + k_{13})n_1 \tag{5}$$

$$\frac{d\,n_2}{dt} = \dot{n}_2 = k_{21}n_1 - (k_{20} + k_{21} + k_{23})n_2, \tag{6}$$

and the quantum efficiency is given by:

$$\eta = \frac{k_{20}n_2}{k_{01}n_0}. \tag{7}$$

If a steady state is assumed, that is $\dot{n}_1$ and $\dot{n}_2$ are equal to zero, the quantum effieciency of the fluorescence intensity can be written:

$$\eta = \frac{k_{20}n_0}{(k_{10} + k_{13} + k_{12})\frac{n_2}{k_{12}}(k_{20} + k_{21} + k_{23}) - k_{12}n_2}$$

$$\eta = \frac{1}{1 + \frac{k_{23}}{k_{20}} + \frac{(k_{10} + k_{13})(k_{20} + k_{21} + k_{23})}{k_{12}k_{20}}}$$

$$\eta = \frac{1}{1 + \beta}. \tag{8}$$

The temperature dependence of the rate constants is given by:

$$k_{23} = k_{23}^{0}\exp(-\frac{E_1}{k_B T}) \tag{9}$$

$$k_{13} = k_{13}^{0}\exp(-(\frac{E_1 - E_2}{k_B T})) \tag{10}$$

$$k_{21} = k_{12}\exp(-\frac{E_2}{k_B T}), \tag{11}$$

with

E_1 being the energy difference between levels 2 and 3

E_2 being the energy difference between levels 1 and 2.

Assuming that $k_{12} > k_{10} > k_{13}$, that is that k_{12} is the fastest was for an electron to leave level 1, β becomes:

$$\beta = \frac{k_{23}}{k_{20}} + \frac{k_{10}}{k_{20}k_{12}}(k_{20} + k_{21} + k_{23})$$

$$\beta = \frac{k_{10}}{k_{12}} + (\frac{k_{23}^{0}}{k_{20}} + \frac{k_{10}k_{23}^{0}}{k_{20}k_{12}})\exp(-\frac{E_1}{k_B T}) + \frac{k_{10}}{k_{20}}\exp(-\frac{E_2}{k_B T})$$

$$\beta = K_1\exp(-\frac{E_1}{k_B T}) + K_2\exp(-\frac{E_2}{k_B T}), \tag{12}$$

with

$$K_1 = \frac{k_{23}^0}{k_{20}} \tag{13}$$

$$K_2 = \frac{k_{10}}{k_{20}}. \tag{14}$$

Thus this model gives two time dependent exponential terms to explain the thermal quenching. In contrast the two level model gives only one exponential term. This equation for the relative quantum efficiency was computer fitted to the fluorescence intensity data and is plotted as a solid line along with the data in Figure 11. The computer program mentioned in Chapter II was used. Also in Figure 9 is a fit to the lifetimes of the proton irradiated SrO. The fitted relative quantum efficiency parameters are listed on the following page in Table I along with values obtained by Jeffries and Summers et al. (12) for proton irradiated SrO. The values listed are comparable. From the lifetime data k_{20} is found to be approximately 2×10^6 s^{-1}. This value coupled with a value of 407 for K_1 makes k_{23}^0 approximately equal to 10^9 s^{-1} which is acceptable for a preexponential coefficient. With the value of 0.950 for K_2, k_{10} is almost equal to k_{20}. This value does not seem of the right magnitude for a nonradiative process. One way the recombination can take place is through direct recombination with the ground level by the production of phonons. Another way is if the electron can be excited to a state where the relaxed $^2A_{1g}^*$ state is very close to the $^2A_{1g}$ ground state, the electron can easily recombine with the ground state.

The model predicts that only from thermal excitation from level 2

TABLE I

QUANTUM EFFICIENCY PARAMETERS

Method/Method Irradiated	E_1(eV)	E_2(eV)	K_1	K_2
Photoluminescence/ Neutron	0.044	0.004	407	0.950
Photoluminescence/ Proton	0.049[a]	0.004[a]	362[a]	0.554[a]
Lifetime/ Proton	0.057[a]	0.007[a]	579[a]	1.260[a]

[a]Reference 12.

to the conduction band does photoconductivity take place. This is because of the relative sizes of k_{23}^{0} and k_{13} and because $k_{12} > k_{10} > k_{13}$. Because levels 1 and 2 are almost degenerate the nonradiative recombination to the ground state from level 1 occurs at low temperatures thus producing the first stage of thermal quenching. Photoconductivity, then, is responsible for the second stage of the thermal quenching. This has been verified (1).

The computed value for E_1 is 0.044 eV. The theoretical value of 0.2 eV and the value obtained by photoconductivity of 0.12 eV cannot be reconciled at this time. The computed value for E_2 is 0.004 eV. This does not seem acceptable since the calculated value is 0.06 eV, but it becomes acceptable because when the Jahn-Teller energy was added to the value of the energy separation of the excited states they almost became degenerate.

In conclusion, the three level model behaves in the following manner. Because of the relatively large magnitude of k_{12}, at low temperatures almost all of the electrons return to the ground state from level 2 producing optical radiation. As the temperature rises an increasing number nonradiatively recombine with the ground state from level 1. Then around 60 K electrons can be thermally excited into the conduction band causing the second stage of thermal decay of the fluorescence intensity. Also photoconductivity can increase rapidly during this second stage. The structure of the model is in accord with the theoretical model and explains the photoconductivity previously seen. It does not explain how the electrons thermally excited into the conduction band recombine with the ground state. Further studies could be

made to look for bleaching or long lived phosphorescence although neither were seen in this experiment. The value of E_1 needs further study also.

A SELECTED BIBLIOGRAPHY

1. Feldott, J. and G. P. Summers, Phys. Rev. B 15, 2295 (1977).

2. Feldott, J., G. P. Summers, T. M. Wilson, H. T. Tohver, M. M. Abraham, Y. Chen, and R. F. Wood, Solid State Commn. 25,839 (1978).

3. Johnson, B. P. and E. B. Hensley, Phys. Rev. 180, 931 (1969).

4. Crawford, J. H. Jr., Private Commn. (1979).

5. Wyckoff, R. W. G., Crystal Structures, Vol. I, II (Interscience Publishers, New York, 1963).

6. American Institute of Physics Handbook (McGraw-Hill Book Co., New York, 1959).

7. Brown, F. C., The Physics of Solids (W. A. Benjamin, Inc., New York, 1967).

8. Bessent, R. G., B. C. Cavenett, and I. C. Hunter, J. Phys. Chem. Solids 29, 1523 (1968).

9. Modine, F. A., E. H. Izen, and J. C. Kemp, Phys. Ltrs. 34A, 413 (1971).

10. Modine, F. A., Y. Chen, R. W. Major, and T. M. Wilson, Phys. Rev. B 14, 1739 (1976).

11. Hughes, A. E. and A. P. Webb, Solid State Commn. 13, 167 (1973).

12. Jeffries, B. T., G. P. Summers, J. Feldott, H. T. Tohver, and Y. Chen, to be published in Phys. Rev. B.

13. Feldott, J., (Ph.D. Dissertation, 1977).

VITA[2]

Bryce T. Jeffries

Candidate for the Degree of

Master of Science

Thesis: AN EXPERIMENTAL INVESTIGATION OF THE ELECTRONIC STRUCTURE OF THE F+-CENTER IN SrO

Major Field: Physics

Biographical:

Personal Data: Born in Wichita, Kansas, May 20, 1948, the son of Mr. and Mrs. Milo Jeffries.

Education: Graduated from Cheney High School, Cheney, Kansas, in May, 1966; attended Kansas University, Lawrence, Kansas, from September, 1966, through May, 1969; enrolled at Central State University, Edmond, Oklahoma, September, 1974, graduated with Bachelor of Science degree in Physics in 1976; completed requirements for the Master of Science degree at Oklahoma State University in Physics in December, 1979.

Professional Experience: Graduate teaching assistant spring semester of 1977; maintained Model AN2000 Van de Graaff Accelerator from June, 1977, through June, 1978; graduate research assistant from July, 1978, through December, 1979.